BRAIN
A JOURNAL OF NEUROLOGY

Expanding the spectrum of neuronal pathology in multiple system atrophy

Matthew D. Cykowski,[1] Elizabeth A. Coon,[2] Suzanne Z. Powell,[1] Sarah M. Jenkins,[3] Eduardo E. Benarroch,[2] Phillip A. Low,[2] Ann M. Schmeichel[2] and Joseph E. Parisi[2,4]

See Halliday (doi:10.1093/brain/awv151) for a scientific commentary on this article.

Multiple system atrophy is a sporadic alpha-synucleinopathy that typically affects patients in their sixth decade of life and beyond. The defining clinical features of the disease include progressive autonomic failure, parkinsonism, and cerebellar ataxia leading to significant disability. Pathologically, multiple system atrophy is characterized by glial cytoplasmic inclusions containing filamentous alpha-synuclein. Neuronal inclusions also have been reported but remain less well defined. This study aimed to further define the spectrum of neuronal pathology in 35 patients with multiple system atrophy (20 male, 15 female; mean age at death 64.7 years; median disease duration 6.5 years, range 2.2 to 15.6 years). The morphologic type, topography, and frequencies of neuronal inclusions, including globular cytoplasmic (Lewy body-like) neuronal inclusions, were determined across a wide spectrum of brain regions. A correlation matrix of pathologic severity also was calculated between distinct anatomic regions of involvement (striatum, substantia nigra, olivary and pontine nuclei, hippocampus, forebrain and thalamus, anterior cingulate and neocortex, and white matter of cerebrum, cerebellum, and corpus callosum). The major finding was the identification of widespread neuronal inclusions in the majority of patients, not only in typical disease-associated regions (striatum, substantia nigra), but also within anterior cingulate cortex, amygdala, entorhinal cortex, basal forebrain and hypothalamus. Neuronal inclusion pathology appeared to follow a hierarchy of region-specific susceptibility, independent of the clinical phenotype, and the severity of pathology was duration-dependent. Neuronal inclusions also were identified in regions not previously implicated in the disease, such as within cerebellar roof nuclei. Lewy body-like inclusions in multiple system atrophy followed the stepwise anatomic progression of Lewy body-spectrum disease inclusion pathology in 25.7% of patients with multiple system atrophy, including a patient with visual hallucinations. Further, the presence of Lewy body-like inclusions in neocortex, but not hippocampal alpha-synuclein pathology, was associated with cognitive impairment ($P = 0.002$). However, several cases had the presence of isolated Lewy body-like inclusions at atypical sites (e.g. thalamus, deep cerebellar nuclei) that are not typical for Lewy body-spectrum disease. Finally, interregional correlations (rho $\geqslant$ 0.6) in pathologic glial and neuronal lesion burden suggest shared mechanisms of disease progression between both discrete anatomic regions (e.g. basal forebrain and hippocampus) and cell types (neuronal and glial inclusions in frontal cortex and white matter, respectively). These findings suggest that in addition to glial inclusions, neuronal pathology plays an important role in the developmental and progression of multiple system atrophy.

1 Department of Pathology and Genomic Medicine, Houston Methodist Hospital, 6565 Fannin St Houston, Texas, 77030, USA
2 Department of Neurology, Mayo Clinic, 200 First St. SW, Rochester, Minnesota, 55905, USA
3 Division of Biomedical Statistics and Informatics, Mayo Clinic, 200 First St. SW, Rochester, Minnesota, 55905, USA
4 Department of Laboratory Medicine and Pathology, Mayo Clinic, 200 First St. SW, Rochester, Minnesota, 55905, USA

Correspondence to: Joseph E. Parisi, M.D.,
Division of Anatomic Pathology,
Departments of Laboratory Medicine and Pathology and Neurology, Mayo Clinic,
200 First Street SW,
Rochester,

MN 55905, USA
E-mail: parisi.joseph@mayo.edu

Introduction

Multiple system atrophy (MSA) is a sporadic neurodegenerative disease characterized clinically by cerebellar dysfunction, parkinsonism, and autonomic failure (Gilman *et al.*, 2008; Ubhi *et al.*, 2011). The disease typically begins in the sixth decade of life and is progressive with mean disease duration of 4.5–9.8 years between diagnosis and death (Ozawa *et al.*, 2004; Yoshida, 2007; Brown *et al.*, 2010; Wenning *et al.*, 2013). Consensus diagnostic criteria distinguish MSA with predominant parkinsonism (MSA-P) and predominant cerebellar ataxia (MSA-C); many patients eventually develop features of both MSA-C and MSA-P. Features of autonomic failure, such as orthostatic hypotension and urogenital symptoms, are also required for the diagnosis of 'probable' or 'possible' MSA (Gilman *et al.*, 2008).

The pathological diagnosis of MSA rests on the demonstration of widespread glial cytoplasmic inclusions (GCIs) (Papp *et al.*, 1989) containing filamentous alpha-synuclein (Trojanowski and Revesz, 2007). MSA is therefore an alpha-synucleinopathy, alongside Lewy body-spectrum disorders such as dementia with Lewy bodies and Parkinson's disease (Schulz-Schaeffer, 2010). The presence of GCIs is fairly specific to MSA, but these have been reported occasionally in other conditions such as idiopathic Parkinson's disease (Wakabayashi *et al.*, 2000). The pathological distribution of lesions correlates to MSA-C and MSA-P phenotypes, particularly within the dorsal striatum, substantia nigra pars compacta, Purkinje cell layer of cerebellum, and inferior olive (Jellinger *et al.*, 2005). In these canonical regions, the pathological changes of neuronal loss and gliosis are often evident on haematoxylin and eosin-stained material.

Neuronal pathology in the form of alpha-synuclein-immunoreactive neuronal inclusions without evident neuronal loss has also been demonstrated in MSA outside of canonical regions (Dickson *et al.*, 1999*a*). The topography and frequency of neuronal inclusions in MSA are not as well defined as those of GCIs because neuronal inclusions are thought to be limited in number and distribution relative to GCIs (Miller *et al.*, 2004). Nonetheless, studies focusing on select anatomic regions have identified neuronal inclusions within the basis pontis, striatum, and mesial temporal lobe (Arima *et al.*, 1992), neocortex (Arai *et al.*, 1994), spinal cord (Yoshida, 2007), precerebellar nuclei (Braak *et al.*, 2003*b*) and other brainstem nuclei (Benarroch, 2007). In contrast, neuronal inclusions are thought to be uncommon (or absent) in the thalamus, subthalamic nucleus, ventral horn of the spinal cord, and deep cerebellar nuclei (Ahmed *et al.*, 2012).

Because of the diagnostic importance of GCIs, the majority of studies on MSA to date have focused mainly on this aspect of MSA pathology. There are fewer studies of neuronal pathology, including the interregional relationships between neuronal inclusions in disparate brain regions. Defining the spectrum of neuronal pathology in MSA has important implications for understanding disease pathogenesis and is critical in the interpretation of functional neuroimaging studies that indicate neuronal involvement (Lyoo *et al.*, 2008).

The present study was undertaken with several aims intended to further define the spectrum of neuronal pathology in MSA. The major aim was to define the topography and morphological subtypes of neuronal inclusions in 35 patients with clinical features of MSA, who were evaluated at Mayo Clinic Rochester, and subsequently pathologically confirmed to have MSA at autopsy. The associations of these findings with various clinical measures of disease were examined. A second aim was to assess interregional relationships in pathological burden for widespread brain regions. Such relationships have been addressed in only a few studies and typically only within canonical regions of MSA pathology (Armstrong *et al.*, 2004; Ozawa *et al.*, 2004). A third aim was to determine the frequency of Lewy body-like inclusions in MSA, and their association with relevant clinical findings, as estimates of this pathology have varied substantially across previous studies.

Materials and methods

Case identification and clinical assessment

Patients included in the study were evaluated at Mayo Clinic Rochester between 1991 and 2014. They were identified through the electronic medical record and patient study databases. Pathologic materials were retrieved and clinical characteristics reviewed (independent of pathologic review) with approval of the Mayo Foundation Institutional Review Board. Clinical variables assessed included disease duration, age at onset, symptoms and signs (including oculomotor findings), clinical diagnosis, presence of visual or auditory hallucinations, carbidopa/levodopa response trial and response

(none, modest, good), rapid eye movement behaviour sleep disorder (RBD), and cognitive impairment. The designation of cognitive impairment in this study was based on clinical symptoms and objective testing including the Short Test of Mental Status (STMS) (Tang-Wai *et al.*, 2003), Montreal Cognitive Assessment, and neuropsychometric testing. All but one cognitively impaired patient underwent formal evaluation using one or more of these measures while the additional patient displayed behavioural problems and visual hallucinations that required nursing home placement. The characterization of MSA patients at Mayo Clinic has been described previously (Iodice *et al.*, 2012).

Histological and immunohistochemical procedures

Tissue samples from multiple areas were studied, including superior frontal gyrus with granular frontal isocortex and frontal hemispheric white matter, agranular frontal cortex/motor cortex, parietal and temporal association isocortices, anterior cingulate cortex and corpus callosum (including the angle of the ventricle and caudate in many cases), amygdala, entorhinal cortex, hippocampus including dentate gyrus and subiculum at the level of the lateral geniculate body, basal forebrain and hypothalamus, thalamus, caudate (typically at the level of nucleus accumbens), putamen and globus pallidus (typically at the level of the mammillary body), insula, midbrain, pons, medulla, cerebellum, and when available, spinal cord. Sections were stained with haematoxylin and eosin, modified Bielschowsky silver, or submitted for immunohistochemical studies.

Immunohistochemical studies were performed on a Leica Bond III platform (Leica Microsystems). These included antibodies to alpha-synuclein (Life Technologies, mouse monoclonal, clone LB509, 1:25 titre), beta-amyloid (Dako, mouse monoclonal, clone 6F/3D, 1:250 titre), tau (Thermo Scientific, mouse monoclonal, clone AT8, 1:7500 titre), and TARDBP (ProteinTech, rabbit polyclonal, 1:3000 titre).

Neuropathological assessment of MSA pathology

Alpha-synuclein-immunoreactive inclusions were described as GCIs or neuronal inclusions and their distribution was recorded. Round or globular cytoplasmic neuronal inclusions on alpha-synuclein were recorded as Lewy body-like neuronal inclusions. Semiquantitative assessments of pathologic involvement were also performed in 12 regions of interest, including anterior cingulate cortex, basal forebrain/hypothalamus, corpus callosum, cerebellar white matter, granular frontal cortex, frontal white matter, hippocampus, inferior olive, pontine nuclei, putamen, substantia nigra, and thalamus. The salient pathological features of each MSA case, as well as representative examples of semiquantitative grading across various cases, were reviewed and agreed upon by two authors (M.D.C., J.E.P.).

For putamen, substantia nigra, pontine nuclei, and inferior olive, a four-point grading system (grades 0–III) was adapted to assess olivopontocerebellar atrophy (OPCA)/MSA-C and striatonigral degeneration/MSA-P pathology (Jellinger *et al.*, 2005). For all OPCA and striatonigral degeneration grades

0 = not involved. OPCA grade in the inferior olive was evaluated as 1 = GCIs only; 2 = GCIs with mild gliosis and neuronal loss; and 3 = GCIs with olivary atrophy, moderate/severe gliosis and neuronal loss. Basis pontis OPCA grade was evaluated as 1 = GCIs only; 2 = GCIs with mild gliosis and neuronal loss; ± atrophy; and 3 = GCIs with moderate/severe gliosis, neuronal loss, and atrophy. Striatonigral degeneration grade in putamen was evaluated as 1 = GCIs; ± atrophy and mild gliosis; 2 = GCIs; ± atrophy, and moderate gliosis and neuronal loss; and 3 = GCIs with severe atrophy, gliosis, and neuronal loss. Striatonigral degeneration grade in substantia nigra was evaluated as 1 = GCIs; ± mild atrophy; mild gliosis and neuronal loss; 2 = GCIs with moderate atrophy, neuronal loss and gliosis; and 3 = GCIs with severe atrophy, neuronal loss, and gliosis. In all cases, gliosis was estimated on haematoxylin and eosin stained sections.

For other regions, GCIs in frontal white matter, cerebellar white matter, and corpus callosum were evaluated as 0 = none; 1 = very rare; 2 = moderate; or 3 = numerous (Inoue *et al.*, 1997; Jellinger *et al.*, 2005) (Supplementary Fig. 1). Pathology in granular frontal cortex, anterior cingulate cortex, and hippocampus (CA1–CA4, subiculum, dentate gyrus) were evaluated as 0 = no GCIs or neuronal inclusions; 1 = rare GCIs or rare neuronal inclusions (1–2 per histological section); 2 = moderate neuronal inclusions (1–2 per any 10 high-power fields ($\times 400$ magnification); or 3 = frequent neuronal inclusions (>2 per any 10 consecutive high-power fields). Pathology in basal forebrain/hypothalamus and thalamus were evaluated as 0 = no pathology; 1 = GCIs only; 2 = rare neuronal inclusions (1–2 per entire section); or 3 = conspicuous neuronal inclusions. The median value of the semiquantitative assessments in these 12 regions was computed as a measure of global pathological severity.

Interregional correlations in MSA pathology

To determine interregional correlations in GCI and neuronal inclusion pathology, a matrix of Spearman correlation coefficients was generated using the aforementioned semiquantitative measures. Thresholds to determine correlations of interest were set at rho ⩾ 0.6 or ⩽ − 0.6. This analysis was treated as exploratory and *P*-values were not calculated.

Neuropathological assessment of non-MSA pathology

The presence/absence of Alzheimer's disease neuropathological changes, argyrophilic grain disease, cerebrovascular pathology (vascular brain injury, cranial atherosclerosis, and cerebral amyloid angiopathy), and hippocampal sclerosis were examined using established criteria (Braak *et al.*, 2000; Pao *et al.*, 2011; Montine *et al.*, 2012). Vascular brain injury was assessed as macro- or microscopic and further classified as acute, subacute, or remote. Cerebral atherosclerosis was recorded as grade 0 (none); grade I (0–25% occlusion of lumen); grade II (25–50%); grade III (50–75%); or grade IV (>75%). Cerebral amyloid angiopathy was defined by beta-amyloid immunoreactivity in the wall of leptomeningeal and/or intracortical vessels. Hippocampal sclerosis was defined as

neuronal loss and gliosis in subiculum and hippocampal sector CA1 without significant Alzheimer's disease changes (Nelson *et al.*, 2011; Pao *et al.*, 2011).

Statistical methods for clinicopathological associations

Non-parametric statistical analyses were performed using R version 3.1.1 (R project for statistical computing, Vienna, Austria, 2014) to determine associations between clinical and pathological variables. Two-sided Wilcoxon rank sum testing was used for comparisons of MSA-P and MSA-C patients with respect to the following variables: OPCA grade, striatonigral degeneration grade, age at onset, and disease duration. Spearman correlation analyses were performed to assess for relationships between disease duration and the following variables: OPCA grade, striatonigral degeneration grade, and global pathologic severity.

Two-sided inference testing was also performed to examine clinicopathologic associations for levodopa (L-DOPA) responsiveness, cognitive impairment, and RBD symptoms. L-DOPA responders/non-responders were compared with respect to number of brain regions with globular cytoplasmic/Lewy body-like inclusions and striatonigral degeneration grade (Wilcoxon rank sum tests), as well as in the association between L-DOPA response and presence of globular cytoplasmic/Lewy body-like inclusions in substantia nigra (χ^2 with Yates continuity correction). Cognitively impaired and cognitively intact patients were compared with respect to severity of pathology in the hippocampal region of interest, as well as global pathologic severity (Wilcoxon rank sum tests). The association between cognitive impairment and neocortical globular cytoplasmic/Lewy body-like inclusions was also examined (χ^2 with Yates continuity correction). The association between RBD and Lewy body-like inclusion pathology in any component of periaqueductal grey, dorsal raphe and reticular formation of midbrain/pons, and locus ceruleus was examined (χ^2 with Yates continuity correction). Fisher exact tests were also performed for 2×2 contingency tables with sparse data. A Bonferonni-corrected type I error rate of 0.0035 was applied to these comparisons to control for false positive results in the 14 statistical tests performed.

Results

Clinical characteristics

Demographic and clinical characteristics for each case are listed in Table 1. Patients included 20 males and 15 females with a mean age at death of 64.7 years (SD = 9.17 years; range of 46 to 85 years), mean age at disease onset of 57.7 years, and median duration of disease of 6.5 years (range of 2.2 to 15.6 years, interquartile range, 3.7 years).

The majority of patients had clinical MSA-P (including two patients with designations of predominant parkinsonism and atypical parkinsonism, respectively) ($n = 18$; 51%). Other clinical designations were MSA-C (including one patient designated OPCA) ($n = 13$ patients; 37%), MSA, not otherwise specified (three patients; 9%), and corticobasal syndrome (one patient). Symptoms included ataxia and gait disturbance (83% of patients), dysautonomia (77%), parkinsonism and/or dyskinesia (74%), urinary incontinence (71%), respiratory insufficiency, sleep apnoea, and stridor (51%), and bulbar symptoms (43%). Cognitive impairment was present in less than one-third of patients (31%). Details of cognitive impairment in these patients are provided in Supplementary Table 1. RBD was present in 14 patients (40%) at an average of 7.5 years prior to death. One patient had visual hallucinations.

Topography of neuronal inclusion and GCI pathology

Tables 2 and 3 show the distributions of structures with neuronal inclusion ± GCIs, GCIs without neuronal inclusions, and structures without any inclusions.

GCIs were linear, comma-shaped, globular, or pyramidal-shaped inclusions. Several features regarding GCI topography were notable. In addition to commonly recognized areas of involvement, GCIs were the predominant or sole cellular inclusion in the globus pallidus, lateral thalamus, cerebellar cortex, red nucleus, and oculomotor/trochlear nuclei. In these regions, neuronal inclusions were only rarely seen (oculomotor/trochlear nuclei, globus pallidus, lateral thalamus) or were not identified (red nucleus). GCIs were minimal or absent in spinal cord dorsal funiculi, but more conspicuous in the lateral and ventral funiculi and dorsal and ventral grey horns at the same level. Rare cases had regions with sparse neuronal inclusions but not evident GCIs. These included cornu ammonis, subiculum, amygdala, caudate nucleus, granular frontal and associative neocortices, dorsomedial and periventricular thalamus, nucleus ambiguus, and hypoglossal nucleus. Typically, however, when neuronal inclusions were present in these regions, GCIs also were present. Lastly, GCIs and neuronal inclusions were minimal or absent in the basis pontis, inferior olive, or putamen of patients with severe pathological changes due to extensive neuronal loss and gliosis.

Morphology and frequency of neuronal inclusion pathology

Representative examples of neuronal intranuclear inclusions, perinuclear neuronal cytoplasmic inclusions, cytoplasmic neuronal cytoplasmic inclusions, and combined inclusion types are shown in Fig. 1. In neuronal cytoplasm, skein-like/filamentous, perinuclear, and granular preinclusions were particularly frequent. Neuronal inclusion type was not stereotypic by site although certain regions appeared to have more frequent neuronal intranuclear inclusions (lateral cuneate), combined neuronal intranuclear inclusion/neuronal cytoplasmic inclusions (pontine nuclei), globular cytoplasmic/Lewy body-like inclusions (pontine

Table 1 Clinical findings in 35 MSA patients

Case	Age	Sex	Duration (Years)	Symptoms	Clinical	CI	L-DOPA	RBD	OPCA	SND
1	85	M	7.9	PRK, GT, INCT	MSA	Y	0	–	III	III
2	75	M	2.3	PRK, INCT, DYST, DYSK, RSP FAIL	PRK	Y	1	Y	I	I
3	65	F	7.3	GT, ATX	OPCA	Y		Y	II	I
4	66	F	5.0	DA, DYSPH, ATX, GT, INCT, MYOC	MSA-C	–		–	I	I
5	75	F	3.6	PRK, DYST, DYSK, DA	CBS	–	0	–	I	II
6	56	F	5.8	ATX, DYSARTH	OPCA	–		–	III	I
7	63	F	2.2	DYSARTH, PRK, DA, INCT	MSA-P	–	2	Y	II	II
8	70	M	3.9	GT, PRK, DA, ATX, INCT	MSA-P	–	0	–	I	III
9	53	M	3.6	GT, PRK, ATX, INCT	MSA-P	–	1	–	I	II
10	46	M	6.2	PRK, DA, INCT, ATX, GT, STRID	MSA-C	Y	0	–	II	III
11	65	M	4.8	PRK, DYSPH, DA, STRID	MSA-P	Y	0	Y	I	II
12	63	F	6.0	DA, PRK, ATX, INCT	MSA	–		–	II	II
13	49	M	7.4	DA, INCT, ATX	MSA-C	–		Y	III	I
14	80	M	6.5	PRK, DA, INCT, SLP APN	MSA-P	–	1	–	I	III
15	67	M	8.9	ATX, DA, PRK, INCT, SLP APN, STRID	MSA-C	–		Y	III	II
16	58	M	9.0	PRK, DA, INCT, DYSPH	MSA-P	–	0	–	I	III
17	74	M	4.1	PRK, DA, DSYK	MSA-P	–	1	–	I	III
18	65	M	7.0	ATX, GT, PRK, DA, INCT, STRID, SLP APN	MSA-C	–	0	Y	III	I
19	67	M	6.0	PRK, DA, INCT	MSA-P	–	0	–	II	III
20	56	M	4.6	PRK, DA, GT, INCT, STRID	MSA-P	–	1	–	I	III
21	66	M	4.6	PRK, DA, INCT	MSA-P	–		–	I	III
22	59	M	5.7	ATX, DA, INCT	MSA-C	–		–	III	II
23	51	F	8.7	PRK, DA, INCT, DYSARTH, DYSPH	MSA-P	–	1	–	I	III
24	62	M	12.5	GT, ATX, INCT, STRID, DYSARTH	MSA-C	–		–	III	III
25	60	F	8.3	PRK, DA, DYST, SLP APN	MSA-P	–	1	–	II	II
26	69	F	7.6	PRK, DA, ATX, INCT	MSA-P	–	1	Y	III	II
27	67	F	11.5	ATX, DA, INCT, DYSPH	MSA-C	Y	2	–	III	II
28	65	F	9.7	ATX, GT, PRK, INCT, DYSPH	MSA-C	Y	1	Y	III	II
29	71	M	9.8	PRK, DYST, INCT, DYSPH, SLP APN	ATY. PRK	–	2	–	II	III
30	55	F	8.5	DA, ATX, GT, STRID	MSA-C	Y		–	III	II
31	78	M	15.6	ATX, DA, DYSARTH, SLP APN	MSA-C	Y		Y	III	III
32	81	F	5.9	DA, PRK, STRID	MSA-P	Y		Y	III	III
33	58	F	6.8	DA, PRK, ATX, DYST, STRID	MSA	–	0	Y	III	III
34	68	M	13.9	PRK, DA, INCT, DYSARTH, DYSPH	MSA-P	Y	1	Y	III	III
35	59	F	6.5	DA, PRK, DYST, DYSARTH, DYSPH, INCT, SLP APN, STRID	MSA-P	–	1	Y	III	III

ATX = ataxia; CBS = corticobasal syndrome; CI = cognitive impairment; DA = dysautonomia; DYSARTH = dysarthria; DYSPH = dysphagia; DYSK = dyskinesia; DYST = dystonia; GT = gait disturbance; INCT = urinary incontinence; L-DOPA = carbidopa/levodopa trial with response (0 = none, 1 = fleeting to moderate, 2 = good); MYOC = myoclonus; PRK = parkinsonism; RSP FAIL = respiratory failure; SLP APN = sleep apnoea; SND = striatonigral degeneration pathologic grade (see text); STRID = stridor; Y = symptom present.

nuclei, substantia nigra, basal forebrain/hypothalamus), or perinuclear neuronal cytoplasmic inclusions (pyramidal cells of isocortical laminae III and V). Figure 2 illustrates the spectrum of neuronal pathology across select regions and patients.

The frequencies of neuronal inclusions by regions were as follows: 100% of patients (anterior cingulate cortex, agranular frontal cortex), >90% of patients (pontine nuclei, amygdala, substantia nigra), 75–90% of patients (entorhinal cortex, basal forebrain/hypothalamus, putamen, caudate, inferior olive, granular frontal cortex, insula, associative isocortex, sensory nuclei of the dorsolateral medulla, and dorsal raphe and reticular formation of midbrain), and 50–70% of patients (medial thalamus, medullary reticular formation, nucleus ambiguus and hypoglossal nuclei, cornu ammonis, dentate gyrus, subiculum, locus ceruleus, and periaqueductal gray matter). Less frequent neuronal inclusions were seen in deep nuclei of the cerebellum (47%), subthalamic nucleus (41%), tectum (36%), lateral thalamus (14%), oculomotor/trochlear nuclei (14%), and globus pallidus (9%). Neuronal inclusions were not identified within the red nucleus, mesencephalic nucleus of the trigeminal nerve, or Purkinje cell layer of cerebellar cortex.

A few points regarding neuronal inclusions deserve additional comment. First, when neuronal inclusions in the amygdala were sparse, these typically occurred in larger cells in the central region of the structure, corresponding approximately to the lateral portions of the basal and accessory basal nuclei (Crosby and Humphrey, 1941). With

Table 2 Alpha-synuclein positive pathologic inclusions in subcortical nuclei, mesial temporal, cingulate, and neocortices

	Mesial temporal lobe					Basal ganglia, forebrain, insula						Cingulate and neocortex					Thalamus		
	DG	CA	SUB	ECX	AMY	BF/HY	GP	CD	PT[a]	STN	INS	CNG	CC	GRN	AGR	ASC	MED	LAT	OTH
1	NI	NI	NI	GCI	NA	NI	GCI	NI	NI	NA	GCI	NI	GCI	NI	NA	NI	NA	NA	NA
2	–	NI	GCI	NI	NI	NI	GCI	NI	NI	NA	NA	NI	GCI	GCI	NI	NI	GCI	GCI	NI
3	–	–	–	NI	NI	NI	GCI	NA	NI	NA	NI	NI	GCI	GCI	NI	NI	GCI	GCI	GCI
4	GCI	GCI	NI	NI	NI	NI	GCI	NI	NI	GCI	NI	NI	GCI	NI	NA	NI	GCI	GCI	GCI
5	–	GCI	–	NI	NI	NI	GCI	GCI	NI	GCI	GCI	NI	GCI	GCI	NI	GCI	GCI	GCI	–
6	–	GCI	–	NI	NI	NI	GCI	NI	NI	NA	–	NI	GCI	NI	NA	NI	GCI	GCI	NI
7	–	–	–	GCI	NI	NA	GCI	NI	NI	NA	NI	NI	GCI	NI	NA	GCI	GCI	GCI	–
8	–	–	NI	NI	NI	NI	GCI	NI	NI	GCI	NI	NI	GCI	GCI	NI	GCI	GCI	GCI	–
9	–	GCI	GCI	GCI	NI	NA	GCI	GCI	NI	GCI	GCI	NI	GCI	NI	NA	GCI	GCI	GCI	GCI
10	NI	GCI	GCI	NI	NI	GCI	GCI	NI	NI	GCI	NI	NI	GCI	NI	NA	NI	NI	NA	GCI
11	–	NI	–	NI	NI	NA	GCI	NI	NI	NA	NI	NI	GCI	NI	NA	NI	GCI	GCI	NI
12	–	–	–	GCI	GCI	GCI	GCI	NI	NI	GCI	GCI	NI	GCI	NI	NI	NI	GCI	GCI	NI
13	NI	NI	–	NI	NI	NI	GCI	GCI	NI	GCI	GCI	NA	NA	NA	NA	NA	NA	NA	GCI
14	–	NI	NI	NI	GCI	NI	GCI	NI	NI	GCI	NI	NI	GCI	NI	NI	NI	GCI	GCI	GCI
15	–	–	–	NI	NI	NA	GCI	NA	NI	NA	NI	NI	GCI	NI	NA	NI	NA	NA	NI
16	NI	GCI	NI	NI	NI	NA	GCI	NI	NI	NI	GCI	NI	GCI	NI	NI	NI	GCI	GCI	NI
17	–	NI	–	NI	NI	NI	GCI	NI	GCI	NI	NI	NI	GCI	NI	NI	NI	NI	NI	NI
18	NI	NI	NI	NI	NI	NI	GCI	GCI	GCI	NA	NI	NI	GCI	GCI	NI	GCI	NA	NA	NI
19	NI	NI	GCI	NI	NI	NI	GCI	NI	NI	NI	NA	NI	GCI	NI	NA	NI	NI	GCI	GCI
20	–	GCI	–	NI	NI	GCI	GCI	NI	NI	NA	NI	NI	GCI	NI	NI	NI	NI	GCI	NI
21	NI	NI	NI	NI	NI	NI	GCI	NI	NI	GCI	NI	NI	GCI	NI	NA	NI	NI	GCI	GCI
22	NI	NI	NI	NI	NI	NI	GCI	NI	NI	NI	NI	NI	GCI	NI	NA	NI	NI	GCI	GCI
23	–	–	–	NI	NI	NI	GCI	GCI	GCI	GCI	NI	NI	GCI	NI	NA	NI	NI	GCI	GCI
24	NI	NI	GCI	NI	NI	NA	GCI	NI	NI	NA	NI	NI	GCI	NI	NI	GCI	GCI	GCI	GCI
25	–	NI	NI	NI	NI	NI	GCI	NI	NI	NI	NI	NI	GCI	NI	NA	NI	NA	NA	NA
26	NI	NI	NI	NI	NI	NI	NI	NI	GCI	NI	NI	NI	GCI	GCI	NA	GCI	NI	NI	GCI
27	NI	NI	NI	NI	NI	NI	GCI	NI	NI	GCI	NI	NI	GCI	NI	NI	NI	NI	GCI	NI
28	NI	NI	NI	NI	NI	NI	NI	NI	NI	NI	NA	NI	GCI	NI	NI	NI	NI	GCI	NI
29	NI	NI	NI	NI	NI	NI	GCI	NI	NI	NI	NI	NI	GCI	NI	NI	NI	NI	NI	GCI
30	NI	NI	NI	NI	NI	NI	GCI	NI	NI	GCI	NI	NI	GCI	NI	NI	NI	NI	GCI	NI
31	NI	GCI	GCI	NI	NI	NI	NI	NI	NI	NI	NI	NI	GCI	NI	NI	NI	NI	NI	NI
32	NI	GCI	NI	NI	NI	NI	GCI	NI	GCI	NA	NI	NI	GCI	NI	NA	NI	NA	NA	NA
33	NI	NI	NI	NI	NI	NI	GCI	GCI	GCI	NA	NI	NI	GCI	NI	NI	NI	NI	GCI	GCI
34	NI	NI	NI	NI	NI	NI	GCI	NI	NI	GCI	GCI	NI	GCI	NI	NA	GCI	NI	GCI	NI
35	NI	NI	NI	NI	NI	NI	GCI	NI	GCI	NI	NI	NI	GCI	NI	NI	NI	NI	GCI	NI

NI = neuronal inclusions present (±GCIs in the structure); – = neither neuronal inclusions or GCIs were present; NA = structure(s) not evaluated with alpha-synuclein.
AMY = amygdala; AGR = agranular frontal cortex including M1; ASC = associative isocortex (temporal and parietal); BF/HY = basal forebrain/hypothalamus; CA = cornu ammonis (CA1–CA4); CC = corpus callosum; CD = caudate;
CNG = anterior cingulate cortex; DG = dentate gyrus; ECX = periarchicortex including entorhinal cortex; GCI = GCIs only; INS = insula; GRN = granular frontal cortex of superior frontal gyrus; GP = globus pallidus; LAT = lateral thalamus
including ventrolateral and ventral posterior nuclei; MED = medial thalamus including dorsomedial nucleus; OTH = other thalamic nuclei including lateral dorsal, anterior, periventricular, and intralaminar nuclei; PT = putamen; SUB = subiculum;
STN = subthalamic nucleus.
[a]Patients 17, 23, and 35 had such extensive neuronal loss in the putamen that only rare GCIs could be noted (as in the inferior olive, the reactive gliosis was alpha-synuclein immunonegative).

Table 3 Alpha-synuclein positive pathologic inclusions in the cerebellum and brainstem

	Medulla					Pons			Midbrain						Cerebellum		Other[d]
	RF	DMN	IX/XII	OLV[a]	SNS	LOC	PN	DR/RF	TCT	III/IV	RN	MsV	PAG	SNG	CTX[b]	NCL[c]	
1	NI	GCI	GCI	NI	NI	NI	NI	NI	GCI	NA	NA	GCI	NI	NI	NA	NA	NI
2	NI	NI	NI	GCI	NI	NA	NI	NI	GCI	GCI	GCI	—	NI	NI	NA	NA	NA
3	GCI	GCI	GCI	NI	NI	NI	NI	GCI	NA	NA	NA	GCI	NA	NI	GCI	—	NA
4	NI	NI	NI	NI	NI	NI	NI	NI	GCI	GCI	GCI	—	GCI	NI	GCI	GCI	NI
5	GCI	GCI	NA	GCI	GCI	GCI	NI	GCI	GCI	—	GCI	GCI	—	NI	GCI	—	NA
6	GCI	—	NI	NI	NI	—	NI	NI	NI	—	GCI	—	—	NI	GCI	—	NI
7	NI	GCI	GCI	GCI	NA	GCI	NI	NI	NA	NA	GCI	—	NA	GCI	GCI	—	NI
8	GCI	GCI	NI	NI	GCI	GCI	NI	NI	GCI	NA	GCI	—	GCI	NI	GCI	—	NA
9	NA	NA	NA	NA	NA	GCI	NI	GCI	GCI	NA	GCI	—	GCI	NI	GCI	GCI	NA
10	GCI	GCI	NI	NI	NI	NI	NI	NI	NI	NA	GCI	—	GCI	NI	NA	NA	NA
11	NA	NA	NA	NA	NA	NI	NI	NI	GCI	GCI	GCI	—	GCI	NI	NA	NA	NA
12	GCI	GCI	NI	GCI	NI	GCI	NI	GCI	GCI	—	NA	—	GCI	GCI	NA	NA	NA
13	NI	GCI	GCI	NI	NI	GCI	NI	GCI	GCI	GCI	GCI	—	NI	NI	GCI	—	NA
14	GCI	—	GCI	NI	NI	NA	GCI	NA	NA	NA	NA	NA	NA	NA	GCI	NI	NA
15	NI	NI	NI	NI	NI	NI	NI	NI	NI	GCI	GCI	GCI	GCI	NI	GCI	NI	NA
16	NI	GCI	GCI	NI	NI	GCI	NI	NI	GCI	GCI	NA	—	GCI	NI	GCI	GCI	NA
17	NI	GCI	NI	NI	NI	NI	NI	NI	GCI	—	GCI	—	NI	NI	GCI	NI	NA
18	NI	GCI	NI	NI	NI	NI	NI	NI	GCI	GCI	NA	GCI	NI	NI	GCI	NI	NA
19	NI	NI	NI	NI	NI	GCI	NI	NI	NI	—	GCI	—	NI	NI	GCI	GCI	NA
20	NA	—	NA	NA	NA	NI	NI	NI	NA	—	NA	NA	GCI	NI	GCI	—	NA
21	GCI	GCI	GCI	NI	NI	NI	NI	NI	GCI	GCI	GCI	—	GCI	NI	GCI	—	NA
22	NI	NI	NI	NI	NI	NI	NI	NI	NA	NA	GCI	—	NA	NI	GCI	NI	NI
23	NI	GCI	GCI	NI	GCI	GCI	NI	GCI	GCI	—	GCI	—	GCI	NI	GCI	—	NI
24	GCI	GCI	NI	NI	NI	NA	NI	GCI	NA	NA	GCI	NA	NA	NI	GCI	NI	NI
25	GCI	GCI	GCI	NI	NI	GCI	NI	NI	NI	NA	NA	NA	NA	NA	GCI	NI	NA
26	NI	GCI	NI	NI	GCI	GCI	NI	NI	NI	NI	GCI	—	GCI	NI	GCI	NI	NI
27	GCI	GCI	NI	—	NI	GCI	NI	NI	GCI	GCI	GCI	—	NI	NI	GCI	GCI	NI
28	NI	NI	NI	NI	NI	NI	NI	NI	GCI	GCI	GCI	—	NI	NI	GCI	NI	NI
29	NI	NI	GCI	NI	NI	NI	NI	NI	NI	NI	GCI	—	NI	NI	GCI	NI	NA
30	NI	NI	NI	NI	NI	NI	NI	NI	NI	NA	GCI	GCI	NI	NI	GCI	NI	NI
31	NI	NI	NI	NI	NI	NI	NI	NI	NI	NA	NA	—	NI	NI	GCI	NI	NA
32	NI	NI	GCI	NI	NI	NI	NI	NI	NI	—	NA	—	NI	NI	GCI	—	NA
33	NI	NA	GCI	NI	NI	NA	NI	NI	NA	NA	GCI	NA	NA	NI	GCI	—	NA
34	NI	NI	NI	NI	NI	NI	NI	NI	GCI	GCI	GCI	GCI	NI	NI	GCI	NI	NI
35	NI	NI	NI	NI	NI	GCI	NI	NI	GCI	NI	GCI	—	NI		GCI	NI	NI

NI = neuronal inclusions present (±GCIs in the structure); — = neither neuronal inclusions or GCIs were present; NA = structure(s) not evaluated with alpha-synuclein.
CTX = cerebellar cortex; IX/XII = motor nuclei of cranial nerve IX and/or XII; DMN = dorsal motor nucleus of X; DR/RF = dorsal raphe nuclei and reticular formation of midbrain and pons; LOC = locus ceruleus; OLV = inferior olive; MsV = mesencephalic nucleus and tract of V; NCL = deep nuclei of cerebellum; PAG = periaqueductal grey of midbrain; PN = pontine nuclei; RF = medullary reticular formation; RN = red nucleus; SNS = sensory nuclei of dorsolateral medulla (see text); SNG = substantia nigra; TCT = tectum of midbrain; III/IV = oculomotor and/or trochlear nuclei.
[a]Patient 27 had such extensive neuronal loss in the olive that only alpha-synuclein-immunonegative reactive gliosis was present.
[b]Cells in the internal granule cell layer with a rim of alpha-synuclein immunoreactivity were often seen. These were interpreted as GCIs although the possibility of rare immunopositive neurons in this layer cannot be excluded. Purkinje cell and molecular layer inclusions were never identified.
[c]Patients 15, 22, 28, 30, 31, 34, and 35 had neuronal inclusions in the roof nuclei of the fourth ventricle.
[d]'OTHER' neuronal inclusions were seen in the facial nucleus (Patients 1, 6 and 34), motor nucleus of V (Patients 4 and 27), ventral horn of the spinal cord (Patients 4, 7, 22, 24, 27 and 28), and olfactory bulb (Patients 23, 26, 30, and 35).

increasing alpha-synuclein burden, neuronal inclusions were more widespread in amygdala. Second, neuronal inclusions in basal forebrain were most frequently identified in magnocellular neurons, particularly nucleus basalis of Meynert, including its lateral extension ventral to putamen. Individual cases had neuronal inclusions in the medial septal nucleus, nucleus of the diagonal band, ventral striatum, and islands of small granule cells. Neuronal inclusions were not seen in large neurons of the ventral pallidum. Hypothalamic areas with neuronal inclusions

included mammillary nuclei, lateral hypothalamic area, and in rare cases, supra-optic and paraventricular nuclei. Third, allocortical neuronal inclusions involved all layers of entorhinal cortex in patients with more extensive pathology but sparse neuronal inclusions in pre-α were the most common finding with mild alpha-synuclein burden (Fig. 2). In the hippocampus, neuronal inclusions were typically identified initially in sectors CA2 and CA1. With increasing alpha-synuclein burden, neuronal inclusions were found in granule cells of dentate gyrus, sectors CA3
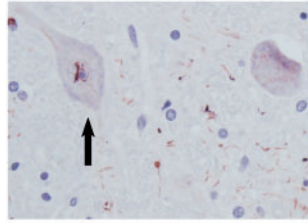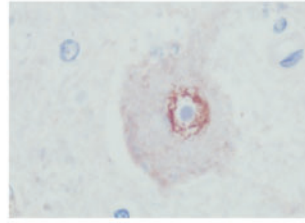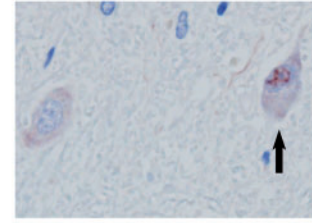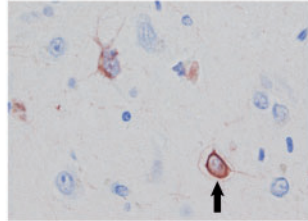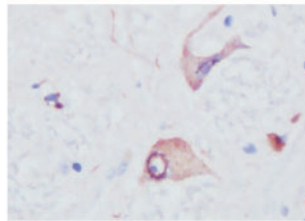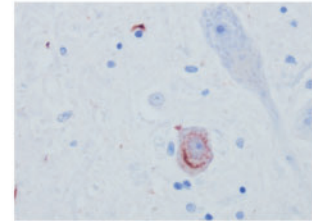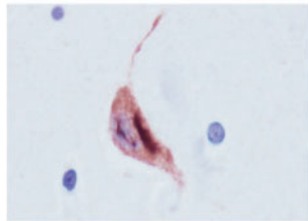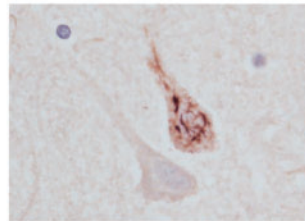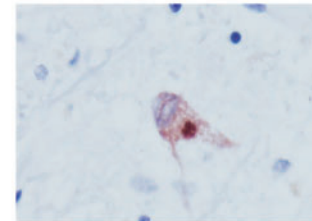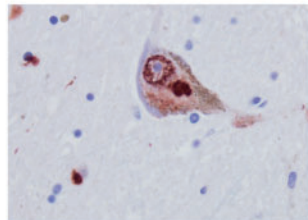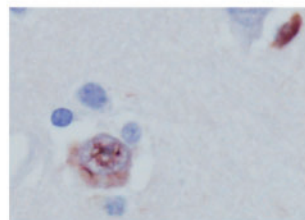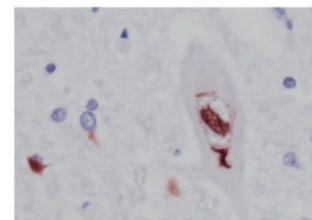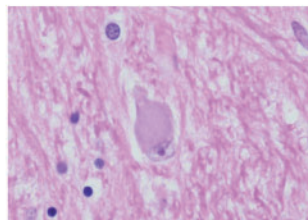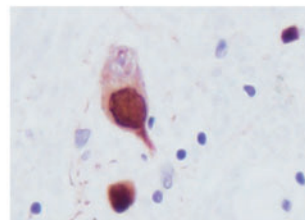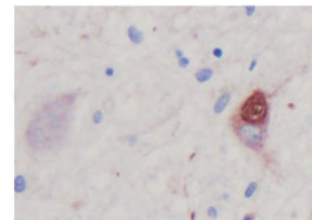
Figure 1 Spectrum of pleomorphic neuronal inclusions in 14 different MSA patients. Alpha-synuclein-immunopositive inclusions are demonstrated in intranuclear (*top row*), perinuclear (*second row*), cytoplasmic (*third row*), and combined intranuclear/cytoplasmic distributions (*fourth row*). The last row shows globular cytoplasmic/Lewy body (LB)-like neuronal inclusions; the haematoxylin and eosin correlates, if present, were pale body-like structures (*left panel of bottom row*). Globular cytoplasmic/Lewy body-like inclusions are shown in the medullary reticular formation (*middle panel of bottom row*) and roof nuclei of cerebellum (*right panel of bottom row*) (see text for details). All images are at ×400. Ctx = cortex; nuc = nucleus; V nuc = motor nucleus of the trigeminal nerve.
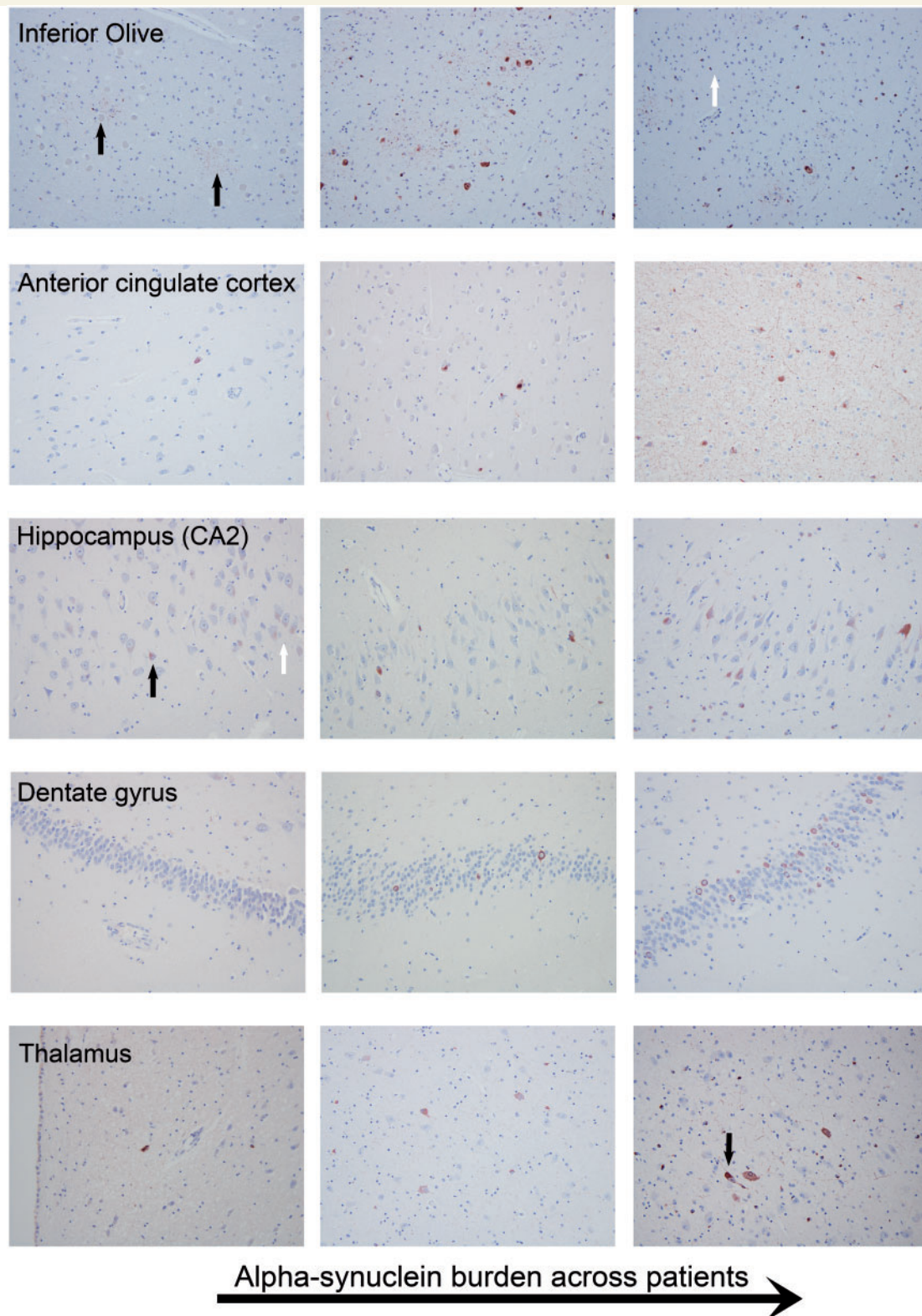
Figure 2 Spectrum of pathologic burden for neuronal inclusions in five regions. Absent/mild to more advanced pathology is shown from left to right for the inferior olive (*top row*), anterior cingulate cortex (*second row*), CA2 sector of hippocampus (*third row*), dentate gyrus of hippocampus (*fourth row*), and thalamic nuclei (*bottom row*). Mild olivary pathology was often associated with plaque-like, immunoreactive processes (*left panel of top row*, black arrows). With advanced olivary pathology, foci of extensive cell loss with immunonegative astrogliosis and absent GCIs and neuronal inclusions were seen (*right panel of top row*, white arrow). For mild CA2 neuronal inclusion pathology, there are rare neuronal inclusions (black arrow, *left panel of third row*) and faint preinclusions (white arrow). A globular cytoplasmic/Lewy body-like neuronal inclusion is seen within a thalamic neuron (black arrow, *right panel of bottom row*) (see text for details). All images are at ×200.

Table 4 'Lewy body-like' cytoplasmic inclusions in 35 MSA patients

	None	RF	DR	DMN	SNS	LOC	PN	SNG	PAG	BFB	INS	AMY	ACC	CA	SUB	ECX	STR	GP	THL	NEO	CRB	OTH
1		+			+	+	+		+				+									+
2										+												
3							+															
4															+							
5								+														
6					+			+														
7		+																				
8							+	+		+												
9		+																				
10											+						+					
11							+												+			
12		+																				
13		+					+	+														
14		+																				
15		+	+	+		+	+							+							+	
16								+														
17								+		+												
18		+	+			+	+		+	+												+
19							+						+									
20								+														
21										+												
22		+	+		+	+	+	+		+		+	+			+						
23		+																				
24							+	+						+								
25		+																				
26		+	+				+	+		+			+	+	+						+	
27		+																				
28		+	+	+	+	+	+	+	+	+		+		+			+	+		+		+
29		+	+		+		+	+		+				+	+				+			
30		+	+	+		+	+	+		+	+	+	+				+	+		+	+	+
31		+	+	+	+	+	+	+	+	+	+	+	+				+	+	+	+	+	+
32		+	+	+		+	+	+		+	+	+	+				+			+		
33		+					+					+	+	+								
34		+	+				+	+		+								+		+	+	
35							+	+		+										+		+

+ = globular cytoplasmic (Lewy body-like) inclusions present.
AMY = amygdala; BFB = basal forebrain/hypothalamus; CA = cornu ammonis; CNG = cingulate cortex; CRB = deep nuclei of cerebellum; DMN = dorsal motor nucleus of X; DR = dorsal raphe; ECX = entorhinal cortex; GP = globus pallidus; INS = insula; LOC = locus ceruleus; NEO = neocortex; OTH = other; PAG = periaqueductal grey; PN = pontine nuclei; RF = reticular formation; SNS = sensory nuclei of dorsolateral medulla; SNG = substantia nigra; SUB = subiculum; THL = thalamus.
The final column, 'other' includes Lewy body-like inclusions that were seen in the tectum (Patient 31), subthalamic nucleus (Patients 28 and 31), olfactory bulb and subcallosal gyrus (Patient 35), hypoglossal nucleus (Patient 18), and facial nucleus (Patient 1).

and CA4, and subiculum. Lastly, neuronal inclusions were found within the median and paramedian cerebellar nuclei (roof nuclei) overlying the fourth ventricle (Supplementary Fig. 2). This finding was present in seven patients with an OPCA pathologic grade of III (Jellinger *et al.*, 2005), five of whom had an MSA-C phenotype.

Frequency and distribution of Lewy body-like neuronal inclusions

Lewy body-like inclusions were defined as circumscribed, globular cytoplasmic inclusions on alpha-synuclein immunostain (with reference to haematoxylin and eosin). Haematoxylin and eosin correlates of these neuronal inclusions, when present, appeared as pale body-like structures and not classic Lewy bodies (Fig. 1).

The anatomical distribution of globular cytoplasmic/ Lewy body-like inclusions is shown in Table 4. This type of neuronal inclusion was very common (80% of MSA patients), occurring in patients with isolated Lewy body-like neuronal inclusions in a single anatomical site as well as in patients with widespread Lewy body-like inclusions. As an example of the former, isolated Lewy body-like inclusions could be seen in thalamus, cerebellar roof nuclei (Fig. 1), striatum, and lateral cuneate nucleus, in the absence of brainstem, amygdala, or cingulate Lewy body pathology. Nine patients (25.7% of all patients studied) showed stepwise progression of globular cytoplasmic/ Lewy body-like inclusions that raised the possibility of

co-existing Lewy body-spectrum disease, based on the presence of these neuronal inclusions in the following areas: medullary reticular formation, ± raphe nuclei, ± dorsal motor nucleus of X, ± loci cerulei, ± pontine nuclei, ± substantia nigra, ± basal forebrain and hypothalamus, ± insula, ± mesial temporal lobe including amygdala, ± cingulate cortex, and ± isocortex (Braak *et al.*, 2003a). Seven of these nine patients had Lewy body-like inclusions in basal forebrain and hypothalamus and the limbic lobe (anterior cingulate cortex, amygdala), respectively. Five of these patients had Lewy body-like inclusions in neocortex.

Non-MSA brain pathology

Supplementary Table 1 details non-MSA pathology in all patients. Briefly, six patients (17.7%) had early Alzheimer's disease neuropathological changes of Braak stage III (*n* = 5) or IV (*n* = 1). These patients had a mean age of 68.5 years at death (SD = 7.09 years). Eight patients (23.5% of cohort) had either no neurofibrillary pathology or minimal neurofibrillary pathology limited to the medial temporal lobe. Argyrophilic grain disease (Braak *et al.*, 2000) was not identified. Parenchymal amyloid plaques were sparse in number and consisted of diffuse plaques (*n* = 9) or diffuse and neuritic plaques (*n* = 6). Vascular pathology included cerebral amyloid angiopathy in seven patients (20.6%) with a mean age of 72 years (SD = 6.88 years). Vascular brain injury was identified in three patients (two with co-existing cerebral amyloid angiopathy) in the form of remote, subacute, or acute infarct(s) (one case per infarct type). Cerebral atherosclerosis was absent in nine patients and mild (grade I–II) in the remainder. Hippocampal sclerosis was present in one patient with cognitive impairment; granule cells of the dentate gyrus in this patient demonstrated dense perinuclear immunoreactivity to both alpha-synuclein and TARDBP.

Clinicopathological correlations

Disease duration was significantly correlated with both global pathological severity (rho = 0.56) and OPCA grade (rho = 0.57). MSA-C and MSA-P patients significantly differed with respect to OPCA grade (*P* = 0.002) though not striatonigral degeneration grade (*P* = 0.008). Cognitive impairment was significantly associated with the presence of Lewy body-like neuronal inclusions in neocortex (Fisher's exact test *P*-value = 0.0014). The remaining comparisons were non-significant, including comparisons of MSA-P and MSA-C patients with respect to age of onset and disease duration.

Interregional correlations in MSA pathology

Figure 3 shows a correlation matrix of Spearman's rho values that represent the interregional correlation in pathological glial and neuronal lesion burden between 12 anatomical
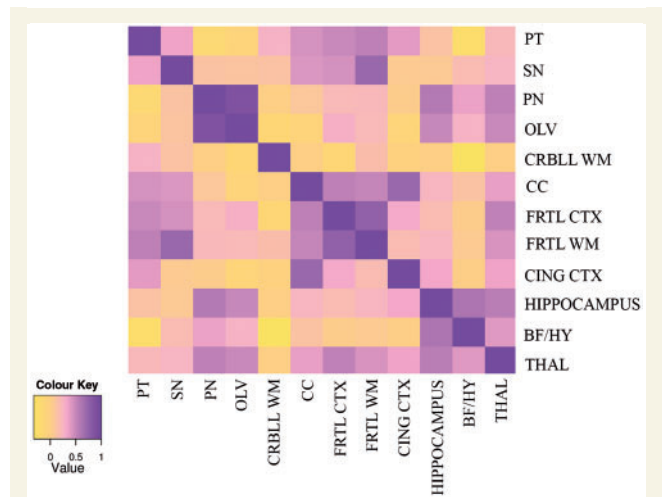

Figure 3 Interregional correlations in alpha-synuclein burden. This is a graphical demonstration of a correlation matrix. Each point in this matrix represents the strength of correlation between the semiquantitative pathologic grading of any two anatomical regions across all patients studied. The colour scale key indicates the strength of the correlation. Dark purple indicates perfect correlation of pathologic severity in two structures (i.e. a Spearman rho correlation coefficient of 1.0 as seen across the diagonal, from top left to bottom right). For instance, pathologic grading in basis pontis (PN) and the inferior olive (OLV) (*row 3, column 4*) is very strongly correlated as indicated by the purple colour (actual Spearman rho value is + 0.88). Conversely, pathological involvement of cerebellar white matter (CRBLL WM) and basal forebrain/hypothalamus (BF/HY) was not correlated at all, as indicated by the yellow colour at row 5, column 11. Other structures evaluated are as follows: putamen (PT), substantia nigra (SN), corpus callosum (CC), anterior cingulate cortex (CING CTX), isocortex of superior frontal gyrus (FRTL CTX), frontal lobe hemispheric white matter (FRTL WM), hippocampus, and thalamus (THAL). Values of Spearman's rho $\geqslant$ 0.6 or $\leqslant$ − 0.6 were of interest in this exploratory analysis (*P*-values were not assigned).

regions as defined above. Each data point in Fig. 3 represents the strength of correlation in pathological grading across all patients studied (a description of semiquantitative grading in these regions is described in the 'Materials and methods' section). These correlations are demonstrated graphically as a heat map with strong correlation represented by dark purple colours and weak or no correlation represented by yellow colours (see also the scale bar in the image). This method provides a way to determine whether the severity of pathological involvement in two different regions is strongly correlated or not [for instance, the severity of glial inclusions in frontal white matter (Fig. 3) and neuronal inclusions in frontal cortex (Fig. 3)].

Interregional correlations in pathological burden exceeding the study threshold (rho $\geqslant$ 0.6 or $\leqslant$ − 0.6) included inferior olive-pontine nuclei (+ 0.88), granular frontal cortex and frontal white matter (+ 0.76), corpus callosum and anterior cingulate cortex (+ 0.71), substantia nigra and frontal white matter (+ 0.71), and hippocampus and basal
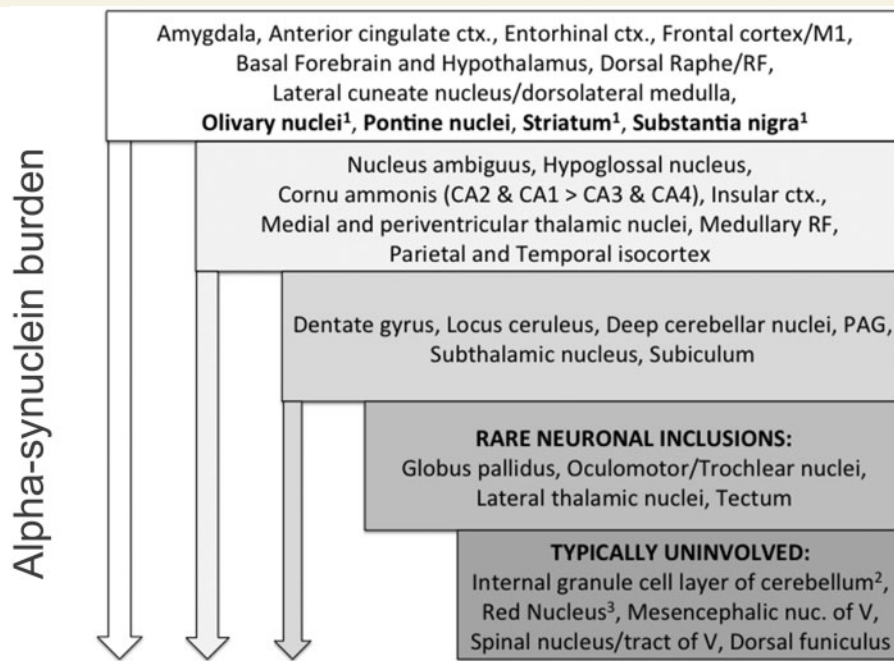
Figure 4 Hierarchy of regional involvement in MSA for 35 patients. The frequency of inclusion pathology is indicated with the most frequent sites of neuronal inclusion pathology in the top tier, including both canonical regions (e.g. pontine nuclei) and non-canonical regions (e.g. anterior cingulate cortex). The downward arrow represents the global increase in alpha-synuclein burden (both glial and neuronal inclusions). In these 35 patients studied, with increasing alpha-synuclein burden (middle and bottom tiers of the hierarchy), additional areas of neuronal pathology could be identified. Some structures, indicated in the two bottom-most tiers, appear to be resistant to neuronal inclusion pathology although glial inclusions were seen. ctx = cortex; RF = medullary reticular formation; PAG = periaqueductal grey of midbrain; nuc = nucleus. 1 = Structures with characteristic neuronal and glial pathology in MSA; 2 = GCIs could be identified but convincing neuronal inclusions were not seen; 3 = GCIs could be identified.

forebrain/hypothalamus ($+0.62$). Negative interregional correlations exceeding -0.6 were not identified.

Discussion

In addition to well recognized GCIs in MSA, widespread neuronal inclusions occur, even at early disease stages. The presence of widespread neuronal inclusions also was independent of MSA-C or MSA-P phenotype. Neuronal alpha-synuclein pathology was seen in regions as diverse as limbic cortex, entorhinal cortex, basal forebrain, hypothalamus, and the roof nuclei of the fourth ventricle. With the exception of the roof nuclei of fourth ventricle, these sites previously have been reported to harbour neuronal inclusions in some patients with MSA; however, the frequency of involvement of regions outside those areas established in striatonigral degeneration and OPCA pathology has not previously been emphasized. This suggests that neuronal pathology in MSA may be more widespread than previously recognized.

The spectrum of neuronal pathology in MSA

A schematic outlining the spectrum of alpha-synuclein pathology across MSA patients, with an emphasis on

neuronal inclusions, is shown in Fig. 4. An important feature of this schematic is that brain regions not typically implicated in MSA (e.g. subthalamic nucleus, dentate nucleus, and periventricular and medial thalamic nuclei) frequently had at least mild neuronal inclusion pathology. Conversely, other brain structures, such as the red nucleus, lateral thalamus, and mesencephalic nucleus of V, rarely (if ever) showed neuronal inclusions, even in the setting of advanced MSA pathology. Further, widespread neuronal inclusions could be identified even in patients with a short course of disease, including cases with neuronal inclusions in regions (cornu ammonis, amygdala, and isocortex) that did not yet have evident GCI pathology. For example, a patient with MSA-P with the shortest disease duration (2.19 years) had neuronal inclusions in amygdala, anterior cingulate, granular frontal isocortex, insula, striatum, granular frontal isocortex, and brainstem, including within pontine nuclei.

This finding of widespread neuronal pathology in MSA is consistent with biochemical studies that have demonstrated pathological soluble alpha-synuclein in widespread brain regions, even in the absence of neuronal inclusions and GCIs (Dickson *et al.*, 1999b). These findings also are consistent with descriptions of neuronal pathology in regions not typically implicated in MSA at early clinical stages (Yoshida, 2007). As demonstrated here, disease duration was significantly correlated with global pathological

severity. This suggests that within different brain regions, there is a progression of alpha-synuclein pathology that is time-dependent; however, the appearance of neuronal inclusions may appear much earlier than previously thought in a number of brain regions. The factors that determine how soluble and diffuse pathological alpha-synuclein subsequently precipitates as immunoreactive inclusions (neuronal inclusions and GCIs) are not entirely understood. Whatever the process, in patients with MSA it may be progressing in multiple brain regions simultaneously, reflected by neuronal inclusions in structurally and functionally disparate brain regions. This also is reflected in analysis of interregional correlation in alpha-synuclein pathology across 12 brain regions. For instance, correlations between increasing neuronal inclusion pathology in regions such as hippocampus and basal forebrain/hypothalamus suggest the possibility of shared pathogenetic mechanisms in these subregions.

These and earlier findings suggest that neurons, along with oligodendroglia, may have an important role in the development of alpha-synuclein pathology in MSA. Although initially affecting a specific vulnerable neuronal system or network (e.g. striatonigral versus olivopontocerebellar), which determines a specific clinical phenotype (MSA-P versus MSA-C), the disease then progresses multifocally. With increasing alpha-synuclein burden, microscopically evident involvement of additional regions, such as dentate gyrus (Arima *et al.*, 1992), may be seen (Fig. 4). A correlation between neuronal pathology and GCIs in striatonigral and olivopontocerebellar regions, suggesting a link between these phenomena, has also been reported (Ozawa *et al.*, 2004), and as in that study, we identified a strong positive correlation between the density of neuronal inclusions (granular frontal cortex) and GCIs (frontal white matter) (Fig. 3). These findings suggest an important relationship between alpha-synuclein accumulation in neuronal inclusions and GCIs, although the mechanisms underlying this remain uncharacterized.

Mesial temporal lobe pathology and cognitive impairment in MSA

Involvement of limbic and allocortical regions was a frequent finding in the patients studied here. For instance, neuronal inclusions were present in amygdala in >90% of patients and in the anterior cingulate cortex of all patients. Hippocampal (Takeda *et al.*, 1997) and parahippocampal cortex neuronal inclusions (Arai *et al.*, 1994) have previously been demonstrated in MSA, but their frequency and distribution is not well characterized. An addition of the present study to these previous descriptions is the demonstration of progressive neuronal pathology in allocortex across MSA patients. The pathological involvement across patients, when present, can succinctly be summarized as neuronal inclusions initially within entorhinal cortex, followed by progression to cornu ammonis (sectors CA2 and

CA1), and then to dentate gyrus granule cells, subiculum, and hippocampal sectors CA3 and CA4.

The spectrum of hippocampal pathology identified here raised questions regarding their potential association with cognitive impairment. Previous studies have shown that 22% of MSA patients are cognitively impaired at initial assessment, whereas nearly 50% of patients surviving more than 8 years have cognitive impairment involving variable domains, including response initiation, perseveration, and memory (Brown *et al.*, 2010). A recent position statement from the Neuropsychology Task Force of the MDS MSA Study Group indicates that cognitive impairment in MSA may be under-recognized, with executive function and verbal fluency most affected, followed by occasional impairments of attention, memory, and visuospatial function, and rarely, language (Stankovic *et al.*, 2014). Fluorodeoxyglucose-PET studies performed at early clinical stages of MSA also have identified a correlation between executive dysfunction/memory impairment and regional cortical hypometabolism (Lyoo *et al.*, 2008), suggesting that these changes may serve as a potential biomarker of disease. In this study, cognitive impairment in MSA was not associated with mesial temporal lobe neuronal pathology, a global measure of neuronal and glial lesion burden, clinical phenotype (MSA-C or MSA-P), or even age at onset. These results are consistent with a recent study by Asi and colleagues (2014), which did not identify any significant differences in the frequency of glial or neuronal pathology in the cortical or limbic regions of cognitively impaired MSA patients.

We did, however, find a significant association between Lewy body-like neuronal inclusions in neocortex and cognitive impairment. This suggests the possibility of neocortical Lewy body-spectrum disease in MSA, although the prevalence of true Lewy body pathology in MSA is currently difficult to estimate (discussed below). One of the patients with cognitive impairment also had TARDBP-positive hippocampal sclerosis (a 78-year-old with Braak stage I neurofibrillary pathology). To our knowledge, TARDBP-positive hippocampal sclerosis has not previously been reported in MSA. The role of alpha-synuclein neuronal inclusions in the hippocampus and dentate gyrus (also frequent in this patient), and their relationship to the unusually long disease duration of this patient (15 years), are not clear. Another patient with cognitive impairment, and without Lewy body-like inclusion pathology, had Braak stage IV neurofibrillary pathology. In general, Alzheimer's disease neuropathology was largely negligible in this population (Supplementary Table 1), consistent with earlier investigations (Jellinger, 2007; Asi *et al.*, 2014).

In summary, there may be multiple pathological substrates of cognitive impairment in MSA. These may include Lewy body-spectrum disease, advanced Alzheimer's disease neuropathology (rarely), or hippocampal sclerosis (rarely). In contrast, TARDBP pathology in MSA is distinctly rare and is not likely to contribute to cognitive impairment (Geser *et al.*, 2011). Other MSA-specific neuronal

pathology, not yet identified, may also contribute to cognitive impairment. A final possibility is that cognitive impairment in MSA is intrinsic to the disease process without an easily discerned neuropathological correlate (Asi *et al.*, 2014).

Involvement of deep cerebellar nuclei in MSA and clinical significance

A finding in this study that has not previously been reported to our knowledge was neuronal pathology in the median and paramedian cerebellar nuclei (cerebellar 'roof' nuclei). These nuclei overlie the fourth ventricle and are difficult to sample due to their small size and ill-defined borders. For this reason they may have been undersampled in previous studies of MSA. Involvement of these nuclei in our study (Supplementary Fig. 2) was seen only with severe OPCA pathology and more commonly in MSA-C patients.

Despite their small size, these roof nuclei are functionally very significant. These cerebellar output nuclei receive input from the cortex of the flocculonodular lobe, and, in the case of the fastigial nucleus, directly from vestibular nuclei itself (Crosby *et al.*, 1962). As such, these are important components of networks involved in balance, posture, and oculomotor control, including smooth pursuit (Robinson *et al.*, 1997). In MSA-C, pathological involvement of midline cerebellum manifests with ataxic gait but also with oculomotor dysfunction (Gilman *et al.*, 2008), which may in part reflect this midline cerebellar pathology. Indeed, all but one of the patients in our cohort with involvement of median and paramedian cerebellar nuclei had oculomotor dysfunction; the most frequent finding was impaired smooth pursuit. There is also increasing evidence that midline cerebellar cortex and deep nuclei participate in non-motor functions, such as control of arterial blood pressure and cognition (Koziol *et al.*, 2014). Deep cerebellar nuclei involvement, particularly within median and paramedian nuclei, may thus contribute to non-motor manifestations of MSA.

Co-occurring Lewy body-spectrum pathology in MSA

Estimates of Lewy body-spectrum disease pathology in MSA have varied across studies (Braak *et al.*, 2003b; Ozawa *et al.*, 2004; Jellinger, 2007). This reflects the inability in many cases to distinguish between true Lewy bodies and Lewy body-like inclusions (Yoshida, 2007). As such, previous authors have used the term 'Lewy body-like' inclusions to describe these lesions (Dickson *et al.*, 1999a). Our study has adopted this term to reflect a similar uncertainty. Further, to avoid potential bias, we chose to record any Lewy body-like neuronal inclusions in all structures surveyed. As there is no method to confidently delineate Lewy body-like inclusions and true Lewy bodies, we subsequently examined whether these followed a pattern of hierarchical progression of Lewy body formation in non-MSA alpha-synucleinopathies (Braak *et al.*, 2003a). For instance, Lewy body-like inclusions might be identified in isolation within pontine nuclei or substantia nigra, but without involvement of other brainstem components (or limbic structures); such cases were recorded as not having co-existing Lewy body-spectrum disease. In those examples, we anticipate these Lewy body-like inclusions reflect a morphological subtype of neuronal inclusion.

This approach, although limited, did identify one patient with extensive Lewy body-like inclusions and visual hallucinations and five patients with neocortical Lewy body-like inclusions (all with cognitive impairment). Hallucinations rarely are reported in MSA (9% of patients) (Stankovic *et al.*, 2014) and whether these represent overlapping Lewy body-spectrum disease is unknown. However, in all five of these patients with neocortical Lewy body-like inclusions there was stepwise involvement of brainstem, limbic structures, and basal forebrain/hypothalamus, as described in non-MSA alpha-synucleinopathies. Between these five patients and others with more limited Lewy body-like inclusions, 25.7% of MSA patients studied had Lewy body-like inclusion pathology that matched the caudal-rostral progression described in Lewy body-spectrum disease. This estimate is consistent with an estimated prevalence of Lewy body-spectrum pathology of 22.7% in MSA (Jellinger, 2007). The frequency of neocortical Lewy body-like inclusions in this study also exceeds that identified in the ageing and cognitively intact population (2.6%) (Knopman *et al.*, 2003). However, the true prevalence of Lewy body-spectrum pathology in MSA may be difficult to ascertain using identification of alpha-synuclein immunoreactive neuronal inclusions. As other authors have pointed out, it is not always possible to accurately discriminate between Lewy bodies and globular cytoplasmic alpha-synuclein-immunoreactive inclusions (Lewy body-like) (Yoshida, 2007).

There are several possibilities that may explain the frequency of Lewy body-like neuronal inclusions in MSA. One possibility is that MSA, as an alpha-synucleinopathy, facilitates formation of globular cytoplasmic/Lewy body-like inclusions in vulnerable neurons of brainstem, amygdala, forebrain, etc. A second possibility is that MSA and dementia with Lewy bodies represent a spectrum disorder, which is conceptually similar to other neurodegenerative diseases such as frontotemporal lobar dementia/amyotrophic lateral sclerosis with TARDBP-positive inclusions (Ravits *et al.*, 2013). The absence of GCIs in the vast majority of non-MSA alpha-synucleinopathies suggests that this is unlikely. A third possibility is that MSA and Lewy body disease, much like the combination of progressive supranuclear palsy and Lewy body disease (Uchikado *et al.*, 2006), represent independent, co-occurring diseases. If indeed these different alpha-synucleinopathies occur as independent and overlapping processes, the frequency of non-specific globular cytoplasmic/Lewy body-like inclusions

in MSA will complicate any pathologically-based estimates of true Lewy body-spectrum disease in these patients.

Implications for disease pathogenesis

At this time the pathogenesis of MSA remains unknown. One possibility is that MSA is a primary gliopathy with neuronal inclusion pathology developing secondarily across the oligo-myelin-axon-neuron complex (Wenning and Jellinger, 2005). Evidence against this hypothesis includes a study in which alpha-synuclein mRNA was not identified in oligodendroglia (Miller *et al.*, 2005). Likewise, other studies have failed to identify an increase in alpha-synuclein mRNA in white matter tracts enriched for GCIs (Ozawa *et al.*, 2001). Conversely, a study by Bleasel and colleagues (2013) found increased mRNA expression of the oligodendrocyte-specific lipid transporter ABCA8 in the involved white and grey matter of patients with MSA. Further, transfection of oligodendroglia with ABCA8 cDNA resulted in upregulation of alpha-synuclein and the myelin-associated protein p25α (Bleasel *et al.*, 2013). An additional study found a non-significant trend toward elevation of the alpha-synuclein-encoding gene *SNCA* in MSA patients (Asi *et al.*, 2014). Relative to our study, we found regions of white matter relatively uninvolved by GCI pathology (e.g. dorsal funiculus of the spinal cord versus involved grey horns and lateral funiculi at the same level) and occasional neuronal inclusions in the absence of detectable GCI pathology (see 'Results' section). These observations would argue against a pathogenetic mechanism that is solely dependent on oligodendroglia in the initial accumulation of pathological alpha-synuclein.

A second possibility is that neuronal and glial inclusions interact synergistically in the degenerative process through as-yet unidentified mechanisms (Yoshida, 2007). In these models, disease progression would result from the simultaneous degeneration of glia and myelin, due to GCIs, and aggregation of alpha-synuclein within neurons (Wakabayashi and Takahashi, 2006). This concept is attractive due to its flexibility; it allows for fibrillar alpha-synuclein to accumulate first in either glia or neurons with either secondary or simultaneous involvement of the remaining components in the oligo-myelin-axon-neuron complex. This potential shared importance of both glial and neuronal inclusions is reflected in the term 'glioneurodegeneration' used by some authors (Stemberger *et al.*, 2010).

A third possibility is that MSA is a neuronal disease and that the formation of GCIs results from secondary accumulation of pathologic alpha-synuclein that is neuronal in origin (Ubhi *et al.*, 2011). In this model, GCI pathology may represent the 'ectopic presence' of abnormal neuronal alpha-synuclein in oligodendroglia (Miller *et al.*, 2005). An experimental study by Reyes and colleagues (2014) provided support for this hypothesis, demonstrating oligodendrocyte uptake of alpha-synuclein from the extracellular environment *in vivo* and *in vitro*, as well as neuron-to-oligodendrocyte transfer of alpha-synuclein. Applying this model to an observational study such as this one, GCIs would be expected to be highest in numbers in association with the projection fibres of regions enriched for neuronal pathology and absent or minimal in oligodendroglia associated with tracts whose origins do not harbour significant neuronal alpha-synuclein accumulation. Here, we did indeed find strong positive correlations between neuronal and glial inclusion pathology (e.g. between frontal cortex and frontal white matter, or between anterior cingulate cortex and corpus callosum white matter). Also, as shown in Fig. 4, our findings do suggest a hierarchy of neuronal vulnerabilities in disparate but stereotypic brain regions, independent of whether pathologic alpha-synuclein first accumulates in neurons. Further, the burden of neuronal pathology increased multifocally as an effect of disease duration and additional regions of anatomical involvement with neuronal inclusions were seen only with increasing overall alpha-synuclein burden.

Our findings emphasize that neuronal pathology in MSA may be more widespread and early than previously recognized. Neuronal inclusion pathology may therefore be a critical component in the development and progression of MSA pathology although the pathogenesis remains unknown at this time. The findings also suggest a gradient of regional involvement with some cell groups frequently involved at very early clinical stages and other cell groups rarely involved, if ever. Further studies are warranted to determine those characteristics that distinguish highly disease-susceptible and disease-resistant neuronal groups in MSA.

Acknowledgements

Funding

Supplementary material

Supplementary material is available at *Brain* online.

References

Ahmed Z, Asi YT, Sailer A, Lees AJ, Houlden H, Revesz T, et al. The neuropathology, pathophysiology and genetics of multiple system atrophy. Neuropathol Appl Neurobiol 2012; 38: 4–24.

Arai N, Papp MI, Lantos PL. New observation on ubiquitinated neurons in the cerebral cortex of multiple system atrophy (MSA). Neurosci Lett 1994; 182: 197–200.

Arima K, Murayama S, Mukoyama M, Inose T. Immunocytochemical and ultrastructural studies of neuronal and oligodendroglial cytoplasmic inclusions in multiple system atrophy. 1. Neuronal cytoplasmic inclusions. Acta Neuropathol 1992; 83: 453–60.

Armstrong RA, Cairns NJ, Lantos PL. A quantitative study of the pathological changes in ten patients with multiple system atrophy (MSA). J Neural Transm 2004; 111: 485–95.

Asi YT, Ling H, Ahmed Z, Lees AJ, Revesz T, Holton JL. Neuropathological features of multiple system atrophy with cognitive impairment. Mov Disord 2014; 29: 884–8.

Asi YT, Simpson JE, Heath PR, Wharton SB, Lees AJ, Revesz T, et al. Alpha-synuclein mRNA expression in oligodendrocytes in MSA. Glia 2014; 62: 964–70.

Benarroch EE. Brainstem respiratory control: substrates of respiratory failure of multiple system atrophy. Mov Disord 2007; 22: 155–61.

Bleasel JM, Hsiao JH, Halliday GM, Kim WS. Increased expression of ABCA8 in multiple system atrophy brain is associated with changes in pathogenic proteins. J Parkinsons Dis 2013; 3: 331–9.

Braak H, Del Tredici K, Bohl J, Bratzke H, Braak E. Pathological changes in the parahippocampal region in select non-Alzheimer's dementias. Ann N Y Acad Sci 2000; 911: 221–39.

Braak H, Del Tredici K, Rub U, de Vos RA, Jansen Steur EN, Braak E. Staging of brain pathology related to sporadic Parkinson's disease. Neurobiol Aging 2003a; 24: 197–211.

Braak H, Rub U, Del Tredici K. Involvement of precerebellar nuclei in multiple system atrophy. Neuropathol Appl Neurobiol 2003b; 29: 60–76.

Brown RG, Lacomblez L, Landwehrmeyer BG, Bak T, Uttner I, Dubois B, et al. Cognitive impairment in patients with multiple system atrophy and progressive supranuclear palsy. Brain 2010; 133: 2382–93.

Crosby EC, Humphrey T. Studies of the vertebrate telencephalon. II. The nuclear pattern of the anterior olfactory nucleus, tuberculum olfactorium and the amygdaloid complex in adult man. J Comp Neurol 1941; 74: 309–52.

Crosby EC, National Institute on Drug Abuse, Addiction Research Center (US). Correlative anatomy of the nervous system. New York: MacMillan; 1962.

Dickson DW, Lin W, Liu WK, Yen SH. Multiple system atrophy: a sporadic synucleinopathy. Brain Pathol 1999a; 9: 721–32.

Dickson DW, Liu W, Hardy J, Farrer M, Mehta N, Uitti R, et al. Widespread alterations of alpha-synuclein in multiple system atrophy. Am J Pathol 1999b; 155: 1241–51.

Geser F, Malunda JA, Hurtig HI, Duda JE, Wenning GK, Gilman S, et al. TDP-43 pathology occurs infrequently in multiple system atrophy. Neuropathol Appl Neurobiol 2011; 37: 358–65.

Gilman S, Wenning GK, Low PA, Brooks DJ, Mathias CJ, Trojanowski JQ, et al. Second consensus statement on the diagnosis of multiple system atrophy. Neurology 2008; 71: 670–6.

Inoue M, Yagishita S, Ryo M, Hasegawa K, Amano N, Matsushita M. The distribution and dynamic density of oligodendroglial cytoplasmic inclusions (GCIs) in multiple system atrophy: a correlation between the density of GCIs and the degree of involvement of striatonigral and olivopontocerebellar systems. Acta Neuropathol 1997; 93: 585–91.

Iodice V, Lipp A, Ahlskog JE, Sandroni P, Fealey RD, Parisi JE, et al. Autopsy confirmed multiple system atrophy cases: mayo experience and role of autonomic function tests. J Neurol Neurosurg Psychiatry 2012; 83: 453–9.

Jellinger KA. More frequent Lewy bodies but less frequent Alzheimer-type lesions in multiple system atrophy as compared to age-matched control brains. Acta Neuropathol 2007; 114: 299–303.

Jellinger KA, Seppi K, Wenning GK. Grading of neuropathology in multiple system atrophy: proposal for a novel scale. Mov Disord 2005; 20 (Suppl 12): S29–36.

Knopman DS, Parisi JE, Salviati A, Floriach-Robert M, Boeve BF, Ivnik RJ, et al. Neuropathology of cognitively normal elderly. J Neuropathol Exp Neurol 2003; 62: 1087–95.

Koziol LF, Budding D, Andreasen N, D'Arrigo S, Bulgheroni S, Imamizu H, et al. Consensus paper: the cerebellum's role in movement and cognition. Cerebellum 2014; 13: 151–77.

Lyoo CH, Jeong Y, Ryu YH, Lee SY, Song TJ, Lee JH, et al. Effects of disease duration on the clinical features and brain glucose metabolism in patients with mixed type multiple system atrophy. Brain 2008; 131 (Pt 2): 438–46.

Miller DW, Cookson MR, Dickson DW. Glial cell inclusions and the pathogenesis of neurodegenerative diseases. Neuron Glia Biol 2004; 1: 13–21.

Miller DW, Johnson JM, Solano SM, Hollingsworth ZR, Standaert DG, Young AB. Absence of alpha-synuclein mRNA expression in normal and multiple system atrophy oligodendroglia. J Neural Transm 2005; 112: 1613–24.

Montine TJ, Phelps CH, Beach TG, Bigio EH, Cairns NJ, Dickson DW, et al. National Institute on Aging-Alzheimer's Association guidelines for the neuropathologic assessment of Alzheimer's disease: a practical approach. Acta Neuropathol 2012; 123: 1–11.

Nelson PT, Schmitt FA, Lin Y, Abner EL, Jicha GA, Patel E, et al. Hippocampal sclerosis in advanced age: clinical and pathological features. Brain 2011; 134 (Pt 5): 1506–18.

Ozawa T, Okuizumi K, Ikeuchi T, Wakabayashi K, Takahashi H, Tsuji S. Analysis of the expression level of alpha-synuclein mRNA using postmortem brain samples from pathologically confirmed cases of multiple system atrophy. Acta Neuropathol 2001; 102: 188–90.

Ozawa T, Paviour D, Quinn NP, Josephs KA, Sangha H, Kilford L, et al. The spectrum of pathological involvement of the striatonigral and olivopontocerebellar systems in multiple system atrophy: clinicopathological correlations. Brain 2004; 127 (Pt 12): 2657–71.

Pao WC, Dickson DW, Crook JE, Finch NA, Rademakers R, Graff-Radford NR. Hippocampal sclerosis in the elderly: genetic and pathologic findings, some mimicking Alzheimer disease clinically. Alzheimer Dis Assoc Disord 2011; 25: 364–8.

Papp MI, Kahn JE, Lantos PL. Glial cytoplasmic inclusions in the CNS of patients with multiple system atrophy (striatonigral degeneration, olivopontocerebellar atrophy and Shy-Drager syndrome). J Neurol Sci 1989; 94: 79–100.

Ravits J, Appel S, Baloh RH, Barohn R, Brooks BR, Elman L, et al. Deciphering amyotrophic lateral sclerosis: what phenotype, neuropathology and genetics are telling us about pathogenesis. Amyotroph Lateral Scler Frontotemporal Degener 2013; 14 (Suppl 1): 5–18.

Reyes JF, Rey NL, Bousset L, Melki R, Brundin P, Angot E. Alpha-synuclein transfers from neurons to oligodendrocytes. Glia 2014; 62: 387–98.

Robinson FR, Straube A, Fuchs AF. Participation of caudal fastigial nucleus in smooth pursuit eye movements. II. Effects of muscimol inactivation. J Neurophysiol 1997; 78: 848–59.

Schulz-Schaeffer WJ. The synaptic pathology of alpha-synuclein aggregation in dementia with Lewy bodies, Parkinson's disease and Parkinson's disease dementia. Acta Neuropathol 2010; 120: 131–43.

Stankovic I, Krismer F, Jesic A, Antonini A, Benke T, Brown RG, et al. Cognitive impairment in multiple system atrophy: a position statement by the Neuropsychology Task Force of the MDS Multiple System Atrophy (MODIMSA) study group. Mov Disord 2014; 29: 857–67.

Stemberger S, Poewe W, Wenning GK, Stefanova N. Targeted over-expression of human alpha-synuclein in oligodendroglia induces lesions linked to MSA-like progressive autonomic failure. Exp Neurol 2010; 224: 459–64.

Takeda A, Arai N, Komori T, Kato S, Oda M. Neuronal inclusions in the dentate fascia in patients with multiple system atrophy. Neurosci Lett 1997; 227: 157–60.

Tang-Wai DF, Knopman DS, Geda YE, Edland SD, Smith GE, Ivnik RJ, et al. Comparison of the short test of mental status and the minimental state examination in mild cognitive impairment. Arch Neurol 2003; 60: 1777–81.

Trojanowski JQ, Revesz T. Proposed neuropathological criteria for the post mortem diagnosis of multiple system atrophy. Neuropathol Appl Neurobiol 2007; 33: 615–20.

Ubhi K, Low P, Masliah E. Multiple system atrophy: a clinical and neuropathological perspective. Trends Neurosci 2011; 34: 581–90.

Uchikado H, DelleDonne A, Ahmed Z, Dickson DW. Lewy bodies in progressive supranuclear palsy represent an independent disease process. J Neuropathol Exp Neurol 2006; 65: 387–95.

Wakabayashi K, Hayashi S, Yoshimoto M, Kudo H, Takahashi H. NACP/alpha-synuclein-positive filamentous inclusions in astrocytes and oligodendrocytes of Parkinson's disease brains. Acta Neuropathol 2000; 99: 14–20.

Wakabayashi K, Takahashi H. Cellular pathology in multiple system atrophy. Neuropathology 2006; 26: 338–45.

Wenning GK, Geser F, Krismer F, Seppi K, Duerr S, Boesch S, et al. The natural history of multiple system atrophy: a prospective European cohort study. Lancet Neurol 2013; 12: 264–74.

Wenning GK, Jellinger KA. The role of alpha-synuclein in the pathogenesis of multiple system atrophy. Acta Neuropathol 2005; 109: 129–40.

Yoshida M. Multiple system atrophy: alpha-synuclein and neuronal degeneration. Neuropathology 2007; 27: 484–93.